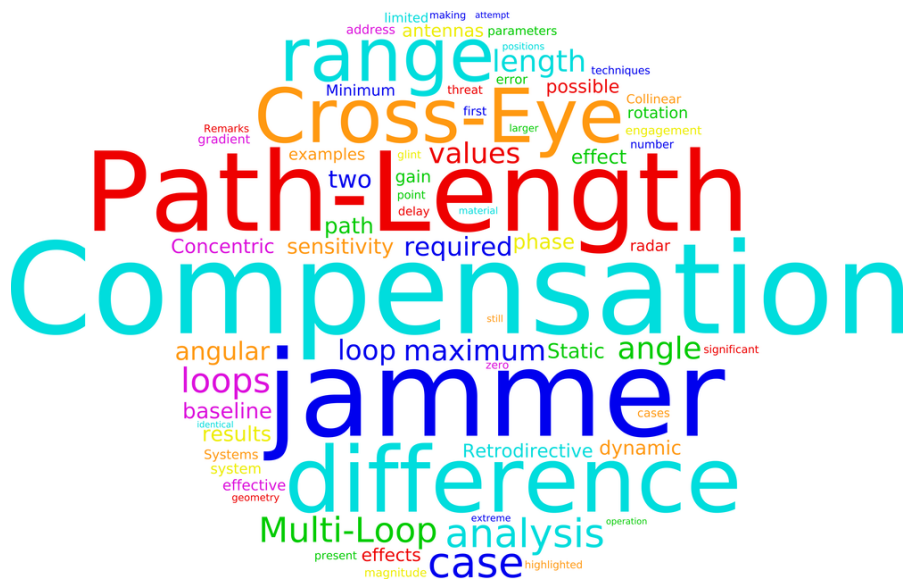


Submitted version of: W. P. du Plessis, "Path-Length Compensation in Multi-Loop Retrodirective Cross-Eye Jamming," *IEEE Transactions on Aerospace and Electronic Systems*, vol. 55, no. 1, pp. 397-406, Feb. 2019. Published version is available online at: <http://ieeexplore.ieee.org/document/8401889>

© 2018 IEEE. Personal use of this material is permitted. Permission from IEEE must be obtained for all other uses, in any current or future media, including reprinting/republishing this material for advertising or promotional purposes, creating new collective works, for resale or redistribution to servers or lists, or reuse of any copyrighted component of this work in other works.



ABBREVIATIONS

- DF direction-finding
- EA electronic attack
- JSR jammer-to-signal ratio
- MAW missile-approach warning
- NRF National Research Foundation of South Africa

Path-Length Compensation in Multi-Loop Retrodirective Cross-Eye Jamming

Warren P. du Plessis, *Senior Member, IEEE*

Abstract—Multi-loop retrodirective cross-eye jammers offer the possibility of both simplifying system implementation and improving system performance. However, the signals for each jammer loop propagate along different paths, leading to potentially detrimental effects on system performance. Static and dynamic compensation for path-length differences are introduced and analysed. Of the two, static compensation is simpler but is only effective for limited engagement geometries. Dynamic compensation is more general but requires an accurate estimate of the engagement geometry.

Index Terms—Cross-eye jamming, multi-loop cross-eye jamming, electronic warfare, and electronic countermeasures.

Manuscript received 27 December 2015; revised 9 April 2016; accepted 17 May 2018. This work is based on the research supported in part by the **National Research Foundation of South Africa (NRF)** (Grant specific unique reference number (UID) 85845). The **NRF** Grantholder acknowledges that opinions, findings and conclusions or recommendations expressed in any publication generated by the **NRF** supported research are that of the author(s), and that the **NRF** accepts no liability whatsoever in this regard.

Warren P. du Plessis is with the University of Pretoria, Pretoria, 0002, South Africa (e-mail: wduplessis@ieee.org).

I. INTRODUCTION

Cross-eye jamming is an **electronic attack (EA)** technique which aims to recreate the worst-case angular error due to glint [1]–[9]. Glint is a naturally-occurring phenomenon which depends only on the characteristics of a radar target, which affects all radar systems and which can lead to large angular errors especially at short ranges [10]. This combination of factors makes cross-eye jamming an extremely attractive self-defence jamming technique, especially in light of the small number of jamming techniques which can induce an angular error in monopulse radars [11], [12].

Despite two patents being filed on cross-eye jamming in 1958 [13], [14], it was only in 2000 that the existence of cross-eye jammers suitable for operational use was first publicly announced [11]. This long delay between the formulation of the concept underlying cross-eye jamming and its successful implementation is due to the practical challenges associated with realising a cross-eye jammer. These challenges are predominantly related to the high **jammer-to-signal ratio (JSR)** required by cross-eye jamming [2]–[5], [15] and the extremely fine matching required of a cross-eye jammer [1]–[7], [16].

Multi-loop cross-eye jamming is the case where multiple cross-eye jammer systems (loops) are used simultaneously. Each jammer loop adds a number of new degrees of freedom to the system both in terms of system geometry (loop positions, rotations, etc.) and electrical parameters (amplitude and phase of each direction through each loop). Previous studies of multi-loop cross-eye jamming have suggested that both the **JSR** requirements and tolerance sensitivity can be reduced [17]–[21], thereby simplifying the implementation of operational cross-eye jammers. Furthermore, the possibility of using a multi-loop cross-eye jammer instead of a number of independent cross-eye jammer loops to increase the performance of a cross-eye jammer as it rotates also exists [21], [22].

While the two signals through a single cross-eye jammer loop travel along identical paths as shown in Fig. 1, the signals through each loop of a multi-loop cross-eye jammer travel along different paths. It has recently been shown these path-length differences can have a major negative effect on system performance of a multi-loop retrodirective cross-eye jammer [23], [24]. Significantly, it was shown that path-length effects can even cause a multi-loop retrodirective cross-eye jammer can act as a beacon, thereby defeating the objective of the jammer by assisting rather than hindering the

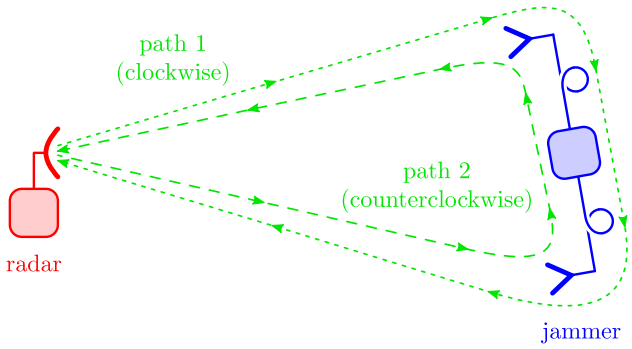


Fig. 1. The paths travelled by the signals through a single-loop retrodirective cross-eye jammer.

threat radar. The implication of the results presented in [23], [24] is thus that multi-loop retrodirective cross-eye jammers may well be of rather limited practical value unless some means to overcome path-length effects can be found.

This paper seeks to address this problem by investigating two possibilities for compensating for path-length differences in multi-loop retrodirective cross-eye jamming. The first possibility is static compensation where different delays (or equivalently, phase shifts) are used for each loop of a multi-loop cross-eye jammer. While static compensation significantly reduces path-length effects, it is not able to provide adequate compensation at high frequencies and over large jammer rotations. Dynamic compensation, where the compensation value is varied according to the engagement geometry, is proposed as a means to overcome the limitations of static compensation. While representing a significant improvement over static compensation, the effectiveness of dynamic compensation may be compromised by inaccurate estimation of the engagement geometry. Those engagement geometries which are most suitable for practical implementation with static and dynamic compensation are identified and evaluated.

The path-length differences between the loops of a multi-loop retrodirective cross-eye jammer are considered in Section II. Compensation for path-length differences is evaluated in Section III by evaluating the extreme values of the path-length differences and the sensitivity to engagement-geometry parameters. A number of examples representative of real-world cross-eye jamming engagements are presented in Section IV. Finally, the main results are summarised in Section V.

II. PATH-LENGTH DIFFERENCES

The path-length differences which result from the use of a multi-loop retrodirective cross-eye jammer are considered below. The first step is the derivation of

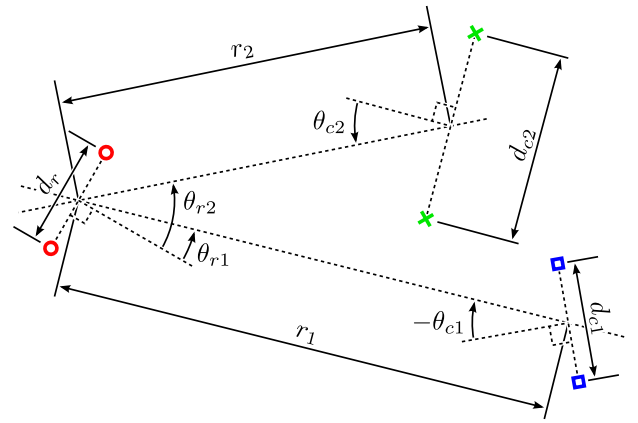


Fig. 2. The geometry of a two-loop cross-eye jamming engagement. The phase centres of the threat radar, and the first and second jammer-loop antennas are denoted by circles, squares and crosses respectively.

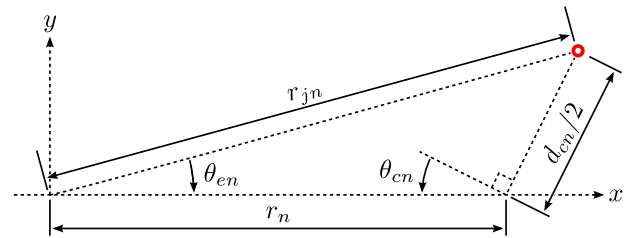


Fig. 3. Computation of the range to each jammer antenna [23].

accurate approximations whose simplified forms allow the relevant issues to be understood and which form the basis of the remainder of this work. These results are then used to investigate the path-length differences encountered in realistic multi-loop cross-eye jamming scenarios with a view to exploring the magnitude of the path-length differences which will be encountered in practice.

A. Analysis

The range to each of the jammer antennas in Fig. 2 can be computed using Fig. 3 giving

$$r_{jn}(\theta_{cn}) = \left[\left(r_n + \frac{d_{cn}}{2} \sin[\theta_{cn}] \right)^2 + \left(\frac{d_{cn}}{2} \cos[\theta_{cn}] \right)^2 \right]^{\frac{1}{2}} \quad (1)$$

$$= \sqrt{r_n^2 + r_n d_{cn} \sin(\theta_{cn}) + \left(\frac{d_{cn}}{2} \right)^2} \quad (2)$$

where the subscript n indicates a parameter of jammer loop n , r_n is the range to the centre of the jammer loop, d_{cn} is the separation of the jammer-loop antennas (the baseline), and θ_{cn} is the jammer-loop rotation. Positive

and negative values of θ_{cn} denote the jammer antennas of loop n which are further from and nearer to the threat radar respectively.

Using a Taylor-series expansion allows (2) to be rewritten as [25]

$$\begin{aligned} r_{jn}(\theta_{cn}) &= \sum_{m=0}^{\infty} \frac{d_{cn}^m}{m!} \times \frac{\partial^m}{\partial d_{cn}^m} r_{jn} \Big|_{d_{cn}=0} \\ &= r_n + d_{cn} \frac{\sin(\theta_{cn})}{2} + d_{cn}^2 \frac{\cos^2(\theta_{cn})}{8r_n} - \\ &\quad d_{cn}^3 \frac{\cos^2(\theta_{cn}) \sin^2(\theta_{cn})}{16r_n^2} - \\ &\quad d_{cn}^4 \frac{\cos^2(\theta_{cn})}{128r_n^3} [5 \cos^2(\theta_{cn}) - 4] + \dots \end{aligned} \quad (3)$$

where the expansion is made around the point $d_{cn} = 0$.¹

The nature of a retrodirective system is that the signal received by the one antenna is retransmitted by the other as shown in Fig. 1, so the total distance travelled by a signal to and from jammer loop n is

$$\begin{aligned} r_{tn} &= r_{jn}(\theta_{cn}) + r_{jn}(-\theta_{cn}) \\ &= 2 \left[r_n + d_{cn}^2 \frac{\cos^2(\theta_{cn})}{8r_n} - \right. \\ &\quad \left. d_{cn}^4 \frac{\cos^2(\theta_{cn})}{128r_n^3} [5 \cos^2(\theta_{cn}) - 4] + \dots \right] \end{aligned} \quad (4)$$

where r_{tn} is the desired result. The total path length (r_{tn}) ignores the delay of the jammer system connecting the two antennas because this delay depends on a number of implementation-specific factors including the hardware components and software processing used. This system delay will be assumed to be identical for all jammer loops in this section to limit the discussion to the effect of the geometrical path-length differences. Section III will show how the system delay can be manipulated to compensate for path-length differences.

The error of a Taylor-series approximation is bounded by the largest magnitude of the smallest-order term which is neglected from the infinite series [25], so

$$r_{tn} \approx 2r_n + \frac{[d_{cn} \cos(\theta_{cn})]^2}{4r_n} \quad (5)$$

with an error less than

$$\Delta r_{tn} \leq \max \left| d_{cn}^4 \frac{\cos^2(\theta_{cn})}{64r_n^3} [5 \cos^2(\theta_{cn}) - 4] \right| \quad (6)$$

$$\leq \frac{d_{cn}^4}{64r_n^3} \quad (7)$$

¹As an aside, the first two terms of the infinite series in (4) constitute the far-field approximation for antennas which is derived using a similar procedure [26].

where Δr_{tn} is the maximum error magnitude possible when computing r_{tn} using (7). For the conservative baseline of 20 m ($d_{cn} = 20$ m) [6] at a range of 1 km ($r_n = 1000$ m), the maximum error obtained using (7) to compute r_{tn} is 2.5 μm which is only 0.12° at 40 GHz. The approximation in (7) is thus extremely accurate for cross-eye jamming scenarios.

Comparing the total distance travelled by the signals for each of the two jammer loops in Fig. 2 shows that the difference is given by

$$r_{t\Delta} = r_{t2} - r_{t1} \quad (8)$$

$$= 2(r_2 - r_1) +$$

$$\frac{1}{4} \left[\frac{[d_{c2} \cos(\theta_{c2})]^2}{r_2} - \frac{[d_{c1} \cos(\theta_{c1})]^2}{r_1} \right]. \quad (9)$$

This range difference ($r_{t\Delta}$) causes a delay difference between the signals of the jammer loops given by

$$\Delta t = \frac{r_{t\Delta}}{c} \quad (10)$$

where Δt is the delay difference and c is the speed of light. This delay difference is equivalent to a phase shift between the jammer loops of

$$\Phi = \beta r_{t\Delta} \quad (11)$$

where Φ is the phase shift and $\beta = 2\pi/\lambda$ is the free-space phase constant with λ being the wavelength. The negative effects of path-length differences on multi-loop cross-eye jammers are a result of this phase difference between the jammer loops [23], [24].

While the above analysis could be extended to include the effect of additional retrodirective cross-eye jammer loops, this addition would not offer additional insight into the underlying issues, while significantly complicating the exposition. The remainder of this document will thus confine itself to the case of two retrodirective cross-eye jammer loops without loss of generality.

B. Examples

A number of examples which highlight specific cases of path-length differences are presented in Table I with both the minimum and maximum path-length differences being provided (see Section III). It should be noted that these cases are slightly optimistic because the larger jammer baseline is on the lower end of the normal range of 10 m to 20 m [6], and a frequency of 3 GHz is low for a tracking radar. Additionally, an angle of 30° between the jammer loops was used, while a value of 90° is recommended by at least one study [22].

It has previously been shown that phase differences close to 180° can cause a retrodirective multi-loop cross-

TABLE I
RANGE DIFFERENCES. JAMMER LOOP 2 HAS A RANGE OF 1 000 M AND A BASELINE OF 10 M.

Case		Jammer 1		Relative	Path Length Difference		Path Phase Difference			
		Range	Baseline	Rotation	Minimum	Maximum	3 GHz		10 GHz	
		(m)	(m)	$\theta_{c2} - \theta_{c1}$	(mm)	(mm)	Minimum	Maximum	Minimum	Maximum
General (Fig. 2)	1	999	5	30°	1 998	2 020	$7 199^\circ$	$7 278^\circ$	$23 998^\circ$	$24 260^\circ$
	2	999	7	30°	1 997	2 016	$7 194^\circ$	$7 262^\circ$	$23 980^\circ$	$24 206^\circ$
	3	999	10	30°	1 994	2 006	$7 182^\circ$	$7 227^\circ$	$23 941^\circ$	$24 091^\circ$
Concentric (Fig. 4)	1	1 000	5	30°	-1.562	20.31	-5.629°	73.18°	-18.76°	243.9°
	2	1 000	7	30°	-3.062	15.81	-11.03°	56.96°	-36.78°	189.9°
	3	1 000	10	30°	-6.250	6.250	-22.52°	22.52°	-75.05°	75.05°
Collinear (Fig. 5)	1	1 000	5	0°	0.000	18.75	0.000°	67.55°	0.000°	225.2°
	2	1 000	7	0°	0.000	12.75	0.000°	45.93°	0.000°	153.1°
	3	1 000	10	0°	0.000	0.000	0.000°	0.000°	0.000°	0.000°

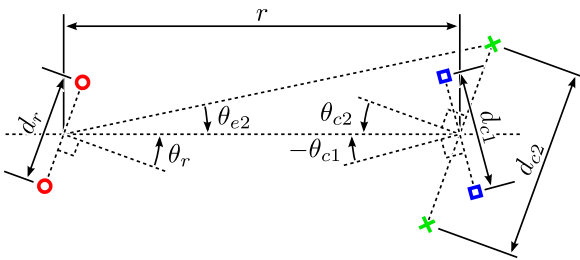


Fig. 4. The change to the geometry in Fig. 2 to ensure that all jammer loops have the same range r (the concentric case) [21], [24].

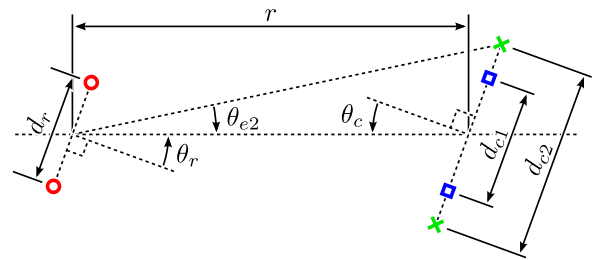


Fig. 5. The change to the geometry in Fig. 4 to ensure that all jammer loops have the same rotation θ_c (the collinear case) [21], [23].

eye jammer to act as a beacon [23], [24], which is precisely the opposite of what a cross-eye jammer seeks to achieve. Furthermore, even in a case where care is taken to minimise the likelihood of beacon operation, a phase difference of greater than 112° can still cause beacon operation [24].

The first three entries in Table I consider the general case shown in Fig. 2. Equation (11) shows that the path-length difference is primarily a result of the range differences between the jammer-loop centres ($r_2 - r_1$) leading to very large differences as a result of the large values of the ranges. Perhaps more importantly, small changes in the relative positions of the jammer loops (e.g. through platform manoeuvre or even just vibration) will lead to significant variations in ranges to the jammer loops and thus the path-length differences. This observation means that it is extremely unlikely that this case will ever find practical application as there is no way to reliably achieve a specified phase difference between the jammer loops. The general case will thus not be considered further in this work.

The concentric case where all jammer loops have

the same range ($r_n = r$) is shown in Fig. 4.² It has been suggested that this case could increase the angular range over which a cross-eye jammer is effective (though without benefit over two independent cross-eye jammers) [21] and could reduce the cross-eye gain variation as the jammer rotates [22]. In this case, (11) shows that the path-length difference is caused by a combination of the differences between the baselines (d_{cn}) and differences between the jammer rotations (θ_{cn}). Table I shows that the path-length difference in the concentric case is significantly smaller than in the general case as a result of the fact that the baselines are orders of magnitude smaller than the ranges ($d_{cn} \ll r_n$). However, the path phase differences are still large enough to compromise the operation of a cross-eye jammer at 10 GHz.

The further requirement that all jammer loops have the same rotation ($\theta_{cn} = \theta_c$) results in the collinear case shown in Fig. 5. This is the case which has been

²This requirement is equivalent to the requirement that all the antenna pairs in a Van-Atta array have coincident centres [27]. However, Van-Atta arrays operate in their far-field region while cross-eye jammers operate in their near-field region [6], so further comparisons between these two retrodirective systems are of only limited value.

considered in the majority of the multi-loop cross-eye jamming literature [17]–[21]. Equation (11) shows that the path-length differences in this case are solely a result of the baseline differences. Table I shows that, while the extreme values are comparable to those for the concentric case, the range of values from the minimum to maximum path-length differences is substantially reduced. The main reason for this reduction is the minimum range difference of 0, which occurs because $r_{tn} = r_n$ when $\theta_{cn} = \pi/2$. Increasing the baseline of the smaller loop reduces both the extreme path-length differences and their variation. Usefully, it has been shown that having multiple loops with similar antenna positions is desirable from the perspective of inducing the largest error in a threat radar [21].

III. PATH-LENGTH COMPENSATION ANALYSIS

Table I clearly demonstrates that the range differences between the loops of a multi-loop cross-eye jammer are large enough to cause significant problems. The discussion thus naturally moves to a consideration of how these path-length differences can be compensated.

Path-length compensation is achieved by modifying the jammer systems connecting the antennas of each jammer loop to compensate for the phase shift between the jammer loops (Φ). This compensation can be implemented either by varying the phase shifts of the jammer systems to compensate for Φ in (13) or by varying the delays through the jammer systems to compensate for Δt in (12).

The first possibility is static compensation where a fixed additional phase shift or delay is introduced into one of the jammer loops. Conceivably, it may even be possible to implement static path-length compensation by simply varying the lengths of the cables used to connect the antennas to the jammer systems. This approach is motivated by the observation that half the difference between the minimum and maximum path-length differences in Table I is small enough to allow reliable jammer operation in many cases. For example, it has been shown that maximum path-length differences of less than 100° can give a minimum cross-eye gain of over 5 [24] resulting in a miss distance of more than 20 m for a 10-m baseline [4]–[7]. However, (11) to (13) show that the required path-length compensation is a function of the engagement geometry, while this approach only implements a fixed compensation value. The implications of this limitation are explored in Section III-A.

The second possibility is dynamic compensation where the compensation applied to the jammer loops is varied according to the engagement geometry. This

approach is motivated by the observation that accurate estimates of the parameters which determine the path-length difference (r_n and θ_{cn}) can allow perfect compensation of path-length differences using (11) to (13). The challenge here is that accurate estimates of all engagement parameters are not always available, and this issue is explored in Section III-B.

A. Static Compensation

Static compensation only implements a single compensation value, so this compensation must be effective over all operating conditions. The optimum compensation value which minimises the maximum path-length difference, and the maximum path-length difference obtained in this way is derived below.

The difference between the jammer rotations is highlighted by defining $\theta_c = \theta_{c2} = \theta_{c1} + \theta_{c\Delta}$, allowing the path-length difference in (11) to be rewritten as

$$r_{t\Delta} = \frac{[d_{c2} \cos(\theta_c)]^2 - [d_{c1} \cos(\theta_c - \theta_{c\Delta})]^2}{4r} \quad (14)$$

because $r = r_n$ in the concentric and collinear cases.

The extreme compensation values required can be obtained from the gradient of the path-length difference ($r_{t\Delta}$) to jammer rotation (θ_c) which is given by

$$\frac{\partial}{\partial \theta_c} r_{t\Delta} = \frac{d_{c1}^2 \sin(2\theta_c - 2\theta_{c\Delta}) - d_{c2}^2 \sin(2\theta_c)}{4r}. \quad (15)$$

The extreme compensation values occur when

$$\frac{\partial}{\partial \theta_c} r_{t\Delta} \Big|_{\theta_c = \theta_{cx}} = 0 \quad (16)$$

$$\tan(2\theta_{cx}) = \frac{d_{c1}^2 \sin(2\theta_{c\Delta})}{d_{c1}^2 \cos(2\theta_{c\Delta}) - d_{c2}^2} \quad (17)$$

$$\theta_{cx} + m \frac{\pi}{2} = \frac{1}{2} \arctan \left[\frac{d_{c1}^2 \sin(2\theta_{c\Delta})}{d_{c1}^2 \cos(2\theta_{c\Delta}) - d_{c2}^2} \right] \quad (18)$$

where θ_{cx} denotes the values of θ_c which give the extreme range-compensation values, and m is any integer. Which of the values of θ_{cx} correspond to the maximum and minimum values of $r_{t\Delta}$ can be determined by substituting (18) into

$$\frac{\partial^2}{\partial \theta_c^2} r_{t\Delta} = \frac{d_{c1}^2 \cos(2\theta_c - 2\theta_{c\Delta}) - d_{c2}^2 \cos(2\theta_c)}{2r} \quad (19)$$

giving

$$\frac{\partial^2}{\partial \theta_c^2} r_{t\Delta} \Big|_{\theta_c = \theta_{cx}} = \pm \frac{\sqrt{d_{c1}^4 + d_{c2}^4 - 2d_{c1}^2 d_{c2}^2 \cos(2\theta_{c\Delta})}}{2r} \quad (20)$$

with the upper and lower signs of the \pm corresponding to even and odd values of m respectively. The minimum

and maximum path-length differences are thus obtained for even and odd values of m respectively.

Substituting jammer rotation values which give the extreme path-length differences (θ_{cx}) into (14) gives

$$r_{t\Delta \min}^{\max} = \frac{1}{8r} \left[d_{c2}^2 - d_{c1}^2 \pm \sqrt{d_{c1}^4 + d_{c2}^4 - 2d_{c1}^2 d_{c2}^2 \cos(2\theta_{c\Delta})} \right] \quad (21)$$

where $r_{t\max}$ and $r_{t\min}$ are the extreme values of $r_{t\Delta}$, and the upper and lower signs of the \pm symbol correspond to $r_{t\max}$ and $r_{t\min}$ respectively. The required path-length compensation is halfway between these extremes giving

$$r_{tc} = \frac{d_{c2}^2 - d_{c1}^2}{4r}. \quad (22)$$

Static compensation is achieved by making the delay or phase through the loop with the narrower baseline longer than the delay or phase through the loop with the wider baseline line by an amount corresponding to r_{tc} . The difference between the extreme path-length differences is given by

$$r_{t\Delta d} = \frac{1}{4r} \sqrt{d_{c1}^4 + d_{c2}^4 - 2d_{c1}^2 d_{c2}^2 \cos(2\theta_{c\Delta})} \quad (23)$$

where $r_{t\Delta d}$ is the path-length difference variation. As outlined above, the largest residual path-length difference which will be achieved with static compensation by r_{tc} is half of the path-length difference variation ($r_{t\Delta d}/2$).

From (21) to (23), it can be seen that the extreme compensation values ($r_{t\Delta \max}$ and $r_{t\Delta \min}$), their difference ($r_{t\Delta d}$) and the compensation delay (r_{tc}) are inversely proportional to the range (r). Additionally, decreasing the baseline of the inner jammer loop (d_{c1}) increases both the compensation required and the residual path-length difference. The combination of range and baseline required for effective static path-length compensation are thus the opposites of the combination of these parameters required for a cross-eye jammer to induce a large angular error in a threat radar [21].

The optimum value of the narrower jammer baseline (d_{c1}) which gives the minimum residual path-length difference ($r_{t\Delta d}/2$) for a multi-loop cross-eye jammer can be computed from

$$0 = \frac{\partial}{\partial d_{c1}} r_{t\Delta d} \quad (24)$$

$$= d_{c1} [d_{c1}^2 - d_{c2}^2 \cos(2\theta_{c\Delta})] \quad (25)$$

$$d_{c1} = d_{c2} \sqrt{\cos(2\theta_{c\Delta})} \quad (26)$$

where solutions $d_{c1} = -d_{c2} \sqrt{\cos(2\theta_{c\Delta})}$ and $d_{c1} = 0$ were discarded because a cross-eye jammer's baseline is positive by definition ($d_{cn} > 0$). The corresponding

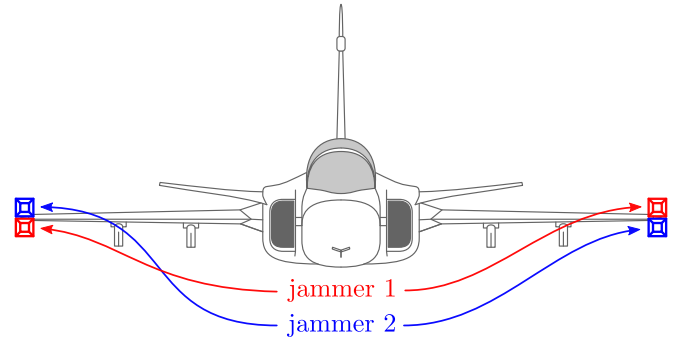


Fig. 6. The placement of multi-loop cross-eye jammer antennas on an aircraft to minimise path-length compensation requirements.

path-length compensation variation is

$$r_{t\Delta d \min} = \left[\frac{d_{c2}}{2} \right]^2 \frac{|\sin(2\theta_{c\Delta})|}{r} \quad (27)$$

with the smallest residual error being half this value.

Observing that the argument of the square-root factor in (21) and (23) can be rewritten as

$$d_{c2}^4 + d_{c1}^4 - 2d_{c2}^2 d_{c1}^2 \cos(2\theta_{c\Delta}) \quad (28)$$

$$= (d_{c2}^2 - d_{c1}^2)^2 + [2d_{c2} d_{c1} \sin(\theta_{c\Delta})]^2 \quad (29)$$

shows that smaller jammer direction differences ($\theta_{c\Delta}$) reduce the path-length compensation requirements. This agrees with Table I where minimum compensation requirements are achieved when the jammer antennas are collinear ($\theta_{c\Delta} = 0$).

Equation 22 shows that no compensation is required ($r_{t\Delta} = 0$) when the jammer antennas are concentric with equal baselines ($r_n = r$ and $d_{cn} = d_c$). Perhaps more significantly, (23) shows that there is no path length difference ($r_{t\Delta d} = 0$) when jammer antennas are collinear and have equal baselines ($r_n = r$, $\theta_{cn} = \theta_c$ and $d_{cn} = d_c$). The optimum jammer-antenna placement to minimise compensation effects for a two-loop retrodirective cross-eye jammer is thus that shown in Fig. 6. However, this case may not always be possible or desirable as a result of other considerations.

An important point to note at this stage is that the extreme-value results derived above are premised on the assumption that the jammer-rotation angles where the extreme range-compensation values are obtained (θ_{cx}) are within the range of jammer-rotation angles over which the jammer is effective (θ_c). For example, extreme values obtained at rotation angles of over 60° ($|\theta_{cx}| > 60^\circ$) are not relevant to a jammer which is only effective over a 120° sector [12] because the jammer rotation is limited to a maximum of 60° ($-60^\circ \leq \theta_c \leq 60^\circ$). Where the required jammer rotation is outside the angular

sector over which the jammer is effective, the values derived above will be conservative in the sense that they overestimate the required compensation.

B. Dynamic Compensation

Dynamic compensation is accomplished by using (11) or (14), and (12) and (13) to determine the amount by which the phase or delay of the jammer loops must be adjusted to compensate for path-length differences. As a result, the sensitivity of the path-length difference to errors in the estimated range and angle of the threat radar (r and θ_c) will determine the effectiveness of dynamic compensation.

This sensitivity (gradient of the path-length difference) to jammer rotation (θ_c) will reach its extreme values when

$$\left. \frac{\partial^2 r_{t\Delta}}{\partial \theta_c^2} \right|_{\theta_c = \theta_{csx}} = 0 \quad (30)$$

$$\tan(2\theta_{csx}) = \frac{d_{c2}^2 - d_{c1}^2 \cos(2\theta_{c\Delta})}{d_{c1}^2 \sin(2\theta_{c\Delta})} \quad (31)$$

$$\theta_{csx} + m\frac{\pi}{2} = \frac{1}{2} \arctan \left[\frac{d_{c2}^2 - d_{c1}^2 \cos(2\theta_{c\Delta})}{d_{c1}^2 \sin(2\theta_{c\Delta})} \right] \quad (32)$$

where θ_{csx} is the value of θ_c at which the sensitivities with the largest magnitudes are obtained. Substituting this value of θ_{csx} into (15) gives

$$\left. \frac{\partial r_{t\Delta}}{\partial \theta_c} \right|_{\theta_c = \theta_{csx}} = \pm \frac{1}{4r} \sqrt{d_{c1}^4 + d_{c2}^4 - 2d_{c2}^2 d_{c1}^2 \cos(2\theta_{c\Delta})} \quad (33)$$

which remarkably, has the same magnitude as the maximum path-length difference ($r_{t\Delta d}$) in (23).

The sensitivity of the path-length difference to range is given by

$$\frac{\partial r_{t\Delta}}{\partial r} = \frac{[d_{c1} \cos(\theta_{c1})]^2 - [d_{c2} \cos(\theta_{c2})]^2}{4r^2}. \quad (34)$$

The angles at which the range sensitivity will be maximised will be the same as the angles at which the path-length difference magnitudes are maximised (θ_{cx}). This is a result of the fact that the values of θ_{cx} maximise magnitude of the numerator of (14) which is identical to the magnitude of the numerator of (34).

IV. EXAMPLES OF PATH-LENGTH COMPENSATION

A number of examples of path-length effects and their compensation are presented in this section to highlight both the value of proposed path-length compensation

techniques and the use of the results derived in Section III.

The feasibility of static path-length compensation is evaluated in Section IV-A by determining the magnitude of the required path-length compensation for a number of cases as the maximum residual path-length difference after static compensation is half this value. The effect of inaccuracies in the estimates of the direction and range to a threat radar are studied in Sections IV-B and IV-C to determine whether dynamic compensation is a practical proposition.

Unless otherwise indicated, the following values of the parameters in Fig. 4 are used to simulate a representative missile threat against an aircraft or ship [7], [8], [23]:

- 3 and 10 GHz threat radar frequencies,
- 1 km engagement range ($r = 1000$ m),
- 5 m smaller jammer baseline ($d_{c1} = 5$ m), and
- 10 m larger jammer baseline ($d_{c2} = 10$ m),
- -30° jammer-rotation difference ($\theta_{c\Delta}$).

These values are considered reasonable, but optimistic in the sense that they will lead to lower compensation values for the following reasons:

- a frequency of 3 GHz is low for a tracking radar, especially in a missile, leading to longer wavelengths and thus smaller phase differences,
- baselines of 10 to 20 m are recommended [6],
- $d_{c1}/d_{c2} = 1/2$ to reduce the compensation values required, whereas a ratio of $d_{c1}/d_{c2} = 1/3$ is used in [18], [20], and
- the worst-case jammer rotations (θ_{cx}) are not considered in all cases.

Note that the discussion below considers path-length compensation with only limited reference to other performance measures. However, the angular error a retro-directive multi-loop cross-eye jammer will induce in a threat radar is considered in detail in [21].

A. Path-Length Difference Magnitudes

The minimum and maximum path-length differences for a number of cases described below are presented in Table II. Providing a static compensation which does not account for the jammer rotation angle (θ_c) inherently implies a maximum compensation error of half the difference between the maximum and minimum values.

The extreme path-length difference results for the default parameters were computed using (21) and (23), and are presented in Table II as Case 1. The maximum static-compensated errors at 3 GHz and 10 GHz for this case are 40.6° and 135.3° respectively. Based on previously-published results [24], this means that static compensation will achieve a minimum cross-eye gain of

TABLE II
EXTREME PATH-LENGTH DIFFERENCE VALUES FOR THE CASES
DESCRIBED IN THE TEXT.

Description	Path-length difference			θ_c
	Distance	3 GHz	10 GHz	
Case 1: Default parameters				
Minimum	-1.89 mm	-6.8°	-22.7°	-83.1°
Maximum	20.64 mm	74.4°	247.9°	6.9°
Difference	22.53 mm	81.2°	270.6°	90.0°
Case 2: Optimum jammer baseline				
Minimum	-4.58 mm	-16.5°	-54.9°	-75.0°
Maximum	17.08 mm	61.5°	205.0°	15.0°
Difference	21.65 mm	78.0°	260.0°	90.0°
Case 3: Limited angular coverage				
Minimum	1.56 mm	5.6°	18.8°	-60.0°
Maximum	20.64 mm	74.4°	247.9°	6.9°
Difference	19.08 mm	68.7°	229.1°	66.9°
Case 4: Case 3 at longer range				
Minimum	0.78 mm	2.8°	9.4°	-60.0°
Maximum	10.32 mm	37.2°	123.9°	6.9°
Difference	9.54 mm	34.4°	114.6°	66.9°
Case 5: Collinear antennas				
Minimum	0.00 mm	0.0°	0.0°	$\pm 90.0^\circ$
Maximum	18.75 mm	67.5°	225.2°	0.0°
Difference	18.75 mm	67.5°	225.2°	90.0°
Case 6: Collinear with limited angular coverage				
Minimum	4.69 mm	16.9°	56.3°	$\pm 60.0^\circ$
Maximum	18.75 mm	67.5°	225.2°	0.0°
Difference	14.06 mm	50.7°	168.9°	60.0°

over 6.5 at 3 GHz, but will not avoid beacon operation at 10 GHz because the maximum residual path-length difference is more than 112°.

The effect of varying the narrower baseline on the maximum path-length difference is shown in Fig. 7. The existence of an optimum value for the smaller baseline is clearly shown at the baseline given by (27). Using this optimum baseline for the smaller jammer loop ($d_{c1} = 7.071$ m) gives the results shown in Table II as Case 2. Comparing Case 2 to Case 1 shows that the reduction in the range of path-length differences is small as anticipated based on Fig. 7. Use of the optimum baseline does thus not make a significant difference to the performance of static path-length compensation.

The range of jammer rotation angles in Cases 1 and 2 stretches up to a maximum of 90° from the broadside direction of the jammer loop with the larger baseline.

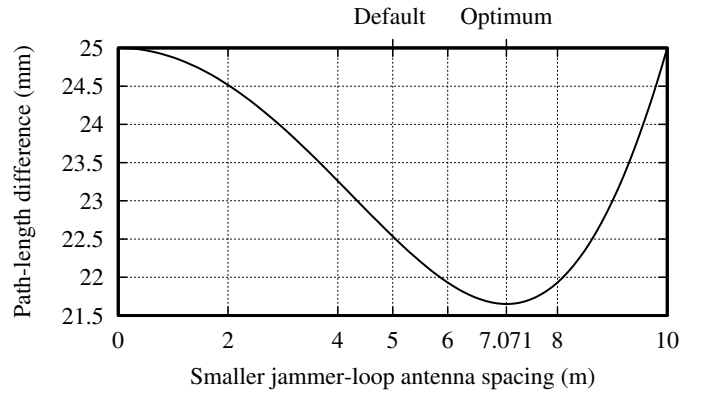


Fig. 7. The path-length difference as a function of the narrower baseline. The specified and optimum values for the smaller jammer baseline are indicated on the top axis.

However, if each jammer loop is assumed to be effective only up to 60° from its broadside direction [12], the range of jammer-rotation angles was thus reduced to extend only from -60° to 30° leading to the results provided in Table II as Case 3.

Comparing Case 3 to Case 1 in Table II shows that the worst-case results in Case 1 are conservative as highlighted in Section III-A. However, the change in the difference between the maximum and minimum path-length differences ($r_{t\Delta d}$) from Case 1 to Case 3 is only 15.3%. The worst-case results thus still provide a useful indication of the performance of static compensation even when narrower angular sectors are considered. That said, it is notable that the maximum path-length phase at 10 GHz is below 112° in Case 3, so beacon operation will be avoided [24].

Section III-A notes that the path-length difference is inversely proportional to the range of an engagement (r). Case 4 in Table II considers Case 3 but at the increased range of 2 km to demonstrate this range dependence. As expected, doubling the range halves the path-length differences, so static compensation which works at a shorter range will also work at a longer range. The smaller path-length phase differences in Case 4 will lead to a minimum cross-eye gain of over 6 even at 10 GHz [24].

As outlined in Section III-A, the use of collinear jammer baselines shown in Fig. 5 will reduce the path-length difference. The one drawback of this approach is that the possibility of using a multi-loop cross-eye jammer to increase the angular coverage of the jammer system is removed, though the other potential benefits of multi-loop cross-eye jamming are retained. Case 5 in Table II considers this possibility when the jammer has an unlimited angular coverage, while Case 6 limits the angular sector to 120° [12].

The use of collinear jammer baselines leads to a significant reduction in the range of path-length differences. Comparing Case 5 to Case 1 and Case 6 to Case 3, shows improvements of 16.8% and 26.3% respectively. Notably, Case 5 has slightly smaller compensation requirements than Case 3 despite the fact that Case 5 considers a much wider angular sector (180° versus 90°). The significantly reduced path-length phase differences in Case 6 mean that minimum cross-eye gains of over 6.5 at 3 GHz and more than 6 at 10 GHz are achieved except at the extreme jammer rotations [24].

The results in Table II show that static compensation can be effective under certain circumstances. The most important consideration is the frequency because lower frequencies have smaller path-length phase differences as a result of their longer wavelengths. Should static compensation not sufficiently reduce path-length differences, the system geometry can be modified by rotating the jammer baselines so that they are closer to collinear ($\theta_{c\Delta} \rightarrow 0$), by adjusting the smaller jammer baseline to its optimal value given by (27), by reducing the larger jammer baseline (d_{c2}), and by increasing the range (r). Unfortunately, each of these options comes at a cost. Collinear baselines mean that the angular coverage of a cross-eye jammer may be decreased, the optimum smaller baseline does not make a large difference, decreasing the larger baseline will reduce the angular error induced in the threat radar, and the range of an engagement is usually not under control of the system designer.

While static path-length compensation will be useful in many cases, it is likely that dynamic path-length compensation will be required by many multi-loop retro-directive cross-eye jammer systems.

B. Effect of Angle-Estimate Inaccuracies

The sensitivity of dynamic path-length compensation to estimates of the jammer rotation angle (θ_c) is crucial to determining the effectiveness of dynamic compensation. A high sensitivity would indicate a requirement for extremely accurate **direction-finding (DF)** systems to provide the necessary estimation accuracy, for example.

As noted in Section III-B, the difference between the maximum and minimum path-length differences ($r_{t\Delta d}$) and the greatest sensitivity of the path-length difference to the jammer rotation angle ($\partial r_{t\Delta}/\partial \theta_c$) have identical magnitudes. Usefully, this means that any changes to the system geometry which reduce the required static compensation will also reduce the sensitivity to angle-estimate inaccuracies. Additionally, this means that the path-length differences in Table II can be reused as the

TABLE III
ANGLE-SENSITIVITY MAGNITUDES FOR THE CASES DESCRIBED
IN THE TEXT.

Sensitivity ($\partial r_{t\Delta}/\partial \theta_c _{\theta_c=\theta_{csx}}$)			
Distance	3 GHz	10 GHz	θ_{csx}
Case 1: Default parameters			
0.39 mm/°	1.4°/°	4.7°/°	-51.9° 38.1°
Case 2: Optimum jammer baseline			
0.38 mm/°	1.4°/°	4.5°/°	-60.0° 30.0°
Case 3: Limited angular coverage			
0.39 mm/°	1.4°/°	4.7°/°	-51.9° 38.1°
Case 4: Case 3 at longer range			
0.20 mm/°	0.7°/°	2.4°/°	-51.9° 38.1°
Case 5: Collinear antennas			
0.33 mm/°	1.2°/°	3.9°/°	-45.0° 45.0°
Case 6: Collinear with limited angular coverage			
0.33 mm/°	1.2°/°	3.9°/°	-45.0° 45.0°

maximum sensitivity of the path-length difference to angular-estimate errors if interpreted as being in units of mm/radian.

The sensitivity magnitudes associated with each of the cases in Table II are presented in Table III with the results being in terms of the phase variation versus angle-estimation error in degrees. The observations for the magnitudes of the results are similar to those for the path-length differences in Table II due to the similarity between the results outlined above.

However, the sensitivities in Table III are small, with the worst value being less than $5^\circ/^\circ$ at 10 GHz. As a result, it should thus be possible to make use of the **DF** system already installed on a platform to perform the angular estimation required for dynamic compensation. For example, even a **DF** angular error of 20° should still avoid beacon operation as a sensitivity of $5^\circ/^\circ$ suggests the path-length difference will be on the order of 100° .

C. Effect of Range-Estimate Inaccuracies

While **DF** techniques are relatively well-established, the same is not true of range estimation from a single platform. This means that range-estimate errors are likely to have a greater effect on the effectiveness of dynamic compensation than the angle-estimate errors considered in Section IV-B.

Table IV lists the sensitivities to range-error estimates obtained using (34) with a 10% range-estimate error for the cases described previously.

The first important observation from Table IV is that the jammer-rotation angles (θ_c) where the maximum

TABLE IV
RANGE-SENSITIVITY MAGNITUDES FOR THE CASES DESCRIBED
IN THE TEXT WITH RANGE ESTIMATION ERRORS OF 10%.

Distance	Sensitivity ($\partial r_{i\Delta}/\partial r _{r=r_0}$)		θ_{cx}
	3 GHz	10 GHz	
Case 1: Default parameters			
2.06 mm/100 m	7.4°/100 m	24.8°/100 m	-6.9°
Case 2: Optimum jammer baseline			
1.71 mm/100 m	6.2°/100 m	20.5°/100 m	-15.0°
Case 3: Limited angular coverage			
2.06 mm/100 m	7.4°/100 m	24.7°/100 m	-6.9°
Case 4: Case 3 at longer range			
1.03 mm/200 m	3.7°/200 m	12.4°/200 m	-6.9°
Case 5: Collinear antennas			
1.88 mm/100 m	6.8°/100 m	22.5°/100 m	0.0°
Case 6: Collinear with limited angular coverage			
1.88 mm/100 m	6.8°/100 m	22.5°/100 m	0.0°

range sensitivity is achieved are well within the range of angles over which a multi-loop cross-eye jammer will be effective. This means that, unlike the other analyses above, the worst-case range sensitivity will be relevant in practice.

While the range sensitivities in Table IV are not large in absolute terms, the inaccuracies associated with range estimation mean that the resulting errors may be great enough to compromise the effectiveness of dynamic compensation.

The similarity between (14) and (34) shows that it is possible to reduce the effect of erroneous range estimates on path-length compensation by making the same changes as those described at the end of Section IV-A in connection with increasing the effectiveness of static compensation. The similarity of the required changes means that both static and dynamic path-length compensation will simultaneously be made more effective. Unfortunately, the same reasons for not wishing to perform the required changes also apply.

The major challenge to achieving effective dynamic path-length compensation thus appears to be the accuracy of the range estimate. This difficulty may be mitigated in some cases by the use of active **missile-approach warning (MAW)** systems which are able to provide accurate ranges of approaching missiles.

V. CONCLUSION

Path-length differences between the loops of a multi-loop retrodirective cross-eye jammer have previously

been shown to potentially have a major detrimental effect on the operation of the jammer system [23], [24]. The compensation of these path-length differences is thus essential to ensure the effectiveness of a multi-loop cross-eye jammer system.

The engagement geometry was shown to determine the path-length differences. The general case where cross-eye jammer loops are arbitrarily positioned leads to large path-length differences which will depend very strongly on the jammer orientation making path-length compensation impractical. Ensuring that the cross-eye jammer loops share a common centre (the concentric case) avoids this problem, but large path-length differences remain. Making the cross-eye jammer loops collinear further reduces the path-length differences, but not enough to make these differences negligible in all cases. The best case is where the antennas of each jammer loop share identical positions as no path-length compensation is required. However, the use of suitable compensation means that this configuration is not an absolute requirement for effective multi-loop retrodirective cross-eye jammer systems.

Path-length compensation is achieved by adjusting the delay and phase of each path through a multi-loop cross-eye jammer relative to the other paths, thereby counteracting for the effects of path-length differences. Static path-length compensation, where the compensation is fixed, appears to be a viable option in cases with a low enough frequency and/or a suitable engagement geometry. However, dynamic compensation, where the compensation is varied according to the engagement geometry, is likely to be required in many cases, particularly where the frequency is high. The effectiveness of dynamic compensation is likely to be dominated by the accuracy of the estimate of the engagement range. The analysis developed allows the determination of whether static or dynamic compensation will be most suitable.

REFERENCES

- [1] S. A. Vakin and L. N. Shustov, "Principles of jamming and electronic reconnaissance – Volume I," U.S. Air Force, Tech. Rep. FTD-MT-24-115-69, AD692642, 1969.
- [2] L. B. Van Brunt, *Applied ECM*. EW Engineering, Inc., 1978, vol. 1.
- [3] A. Golden, *Radar Electronic Warfare*. AIAA Inc., 1987.
- [4] D. C. Schleher, *Electronic warfare in the information age*. Artech House, 1999.
- [5] F. Neri, *Introduction to Electronic Defense Systems*, 2nd ed. Rayleigh, USA: SciTech Publishing, 2006.
- [6] L. Falk, "Cross-eye jamming of monopulse radar," in *IEEE Waveform Diversity & Design Conf.*, Pisa, Italy, 4-8 June 2007, pp. 209–213.
- [7] W. P. du Plessis, "A comprehensive investigation of retrodirective cross-eye jamming," Ph.D. dissertation, University of Pretoria, 2010.

- [8] W. P. du Plessis, J. W. Odendaal, and J. Joubert, "Extended analysis of retrodirective cross-eye jamming," *IEEE Trans. Antennas Propag.*, vol. 57, no. 9, pp. 2803–2806, Sept. 2009.
- [9] W. P. du Plessis, J. W. Odendaal, and J. Joubert, "Experimental simulation of retrodirective cross-eye jamming," *IEEE Trans. Aerosp. Electron. Syst.*, vol. 47, no. 1, pp. 734–740, Jan. 2011.
- [10] J. W. Wright, "Radar glint – a survey," *Electromagnetics*, vol. 4, no. 2, pp. 205–227, Jan. 1984.
- [11] F. Neri, "Experimental testing on cross-eye jamming," in *AOC Int. Symp. Conf.*, Las Vega, USA, 2000.
- [12] F. Neri, "Anti-monopulse jamming techniques," in *Proc. 2001 SBMO/IEEE MTT-S Microw. Optoelectronics Conf.*, vol. 2, 2001, pp. 45–50.
- [13] P. K. Shizume, "Angular deception countermeasure system," U.S.A. Patent 4 117 484, September 26, 1978.
- [14] B. L. Lewis and D. D. Howard, "Security device," U.S.A. Patent 4 006 478, Feb. 1, 1977.
- [15] W. P. du Plessis, "Platform skin return and retrodirective cross-eye jamming," *IEEE Trans. Aerosp. Electron. Syst.*, vol. 48, no. 1, pp. 490–501, Jan. 2012.
- [16] W. P. du Plessis, J. W. Odendaal, and J. Joubert, "Tolerance analysis of cross-eye jamming systems," *IEEE Trans. Aerosp. Electron. Syst.*, vol. 47, no. 1, pp. 740–745, Jan. 2011.
- [17] C. Musso and C. Curt, "Robustness of a new angular countermeasure," in *Radar 97*, 14–16 Oct. 1997, pp. 415–419.
- [18] N. M. Harwood, W. N. Dawber, V. A. Kluckers, and G. E. James, "Multiple-element crosseye," *IET Radar Sonar Nav.*, vol. 1, no. 1, pp. 67–73, Feb. 2007.
- [19] T. Liu, X. Wei, and L. Li, "Multiple-element retrodirective cross-eye jamming against amplitude-comparison monopulse radar," in *Int. Conf. Signal Process. (ICSP)*, HangZhou, China, Oct 2014, pp. 2135–2140.
- [20] T. Liu, D. Liao, X. Wei, and L. Li, "Performance analysis of multiple-element retrodirective cross-eye jamming based on linear array," *IEEE Trans. Aerosp. Electron. Syst.*, vol. 51, no. 3, pp. 1867–1876, July 2015.
- [21] W. P. du Plessis, "Cross-eye gain in multi-loop retrodirective cross-eye jamming," *IEEE Trans. Aerosp. Electron. Syst.*, vol. 52, no. 2, pp. 875–882, April 2016.
- [22] S. Liu, C. Dong, J. Xu, G. Zhao, and Y. Zhu, "Analysis of rotating cross-eye jamming," *IEEE Antennas Wireless Propag. Lett.*, vol. 14, pp. 939–942, Dec 2015.
- [23] W. P. du Plessis, "Path-length effects in multiloop retrodirective cross-eye jamming," *IEEE Antennas Wireless Propag. Lett.*, vol. 15, pp. 626–629, March 2016.
- [24] W. P. du Plessis, "Analysis of path-length effects in multi-loop cross-eye jamming," *IEEE Trans. Aerosp. Electron. Syst.*, vol. 53, no. 5, pp. 2266–2276, Oct. 2017, revision submitted on 4 Jan. 2017.
- [25] R. Ellis and D. Gulick, *Calculus with analytic geometry*, 5th ed. Harcourt Brace & Company, 1994.
- [26] C. A. Balanis, *Antenna theory: analysis and design*, 2nd ed. John Wiley & Sons, Inc., 1997.
- [27] L. C. Van Atta, "Electromagnetic reflector," U.S.A. Patent 2 908 002, Oct. 6, 1959.



Warren du Plessis (M'00, SM'10) received the B.Eng. (Electronic) and M.Eng. (Electronic) and Ph.D. (Engineering) degrees from the University of Pretoria in 1998, 2003 and 2010 respectively, winning numerous academic awards including the prestigious Vice-Chancellor and Principal's Medal.

He spent two years as a lecturer at the University of Pretoria, and then joined Grintek Antennas as a design engineer for almost four years, followed by six years at the Council for Scientific and Industrial Research (CSIR). He is currently an Associate Professor at the University of Pretoria, and his primary research interests are cross-eye jamming and thinned antenna arrays.